Effect of insulation paper ageing on the vibration characteristics of a winding disc

Ming Jin and Jie Pan

School of Mechanical Engineering, University of Western Australia, WA, Australia

ABSTRACT

Vibration analysis has been applied to power transformer condition monitoring in the last few decades. It uses the characteristic vibration of the transformer to detect and diagnose transformer failures. Because the winding insulation paper degradation is a very common and serious power transformer failure, this paper is concerned with the effect of ageing of winding insulation paper on the vibration of a simplified "winding model", comprising a single layer of concentric circular rings wrapped with insulation paper. The insulation paper undertakes high thermal and electrical pressure in an operational transformer, and the average molecular of cellulose chains decreases with age which causes both the insulation abilities and mechanical strength of the paper to degrade. By testing the vibration of the concentric rings with different ageing papers, it is found that the natural frequencies of the rings shift to low frequency end when the mechanical strength of the paper decreases. A mechanical model of the rings with paper is provided here to identify the relationship between the paper mechanical properties with their corresponding vibrations. Based on the work reported in this paper, it is believed that the ageing extent of winding insulation paper can be detected by monitoring the vibration of the winding.

1. INTRODUCTION

The power transformer is one of the most important components in the power industry. Failures of a serving power transformer may cause huge economic loss directly and indirectly. Although the primary power transformer failure is the load tap changer problem (40%) and the power transformers' disc-type winding problem is secondary (15%-20%), the latter failure is much more lethal [1, 2]. Usually, a serious power winding failure is unrepairable, and the only solution is replacing the failed transformer which costs millions of dollars. Therefore, monitoring the performance of power transformer disc-type windings and preventing them from failure is practically significant.

One approach in condition monitoring of power transformers involves detecting transformer winding failures by analysing the characteristic vibration of the winding structure used in last few decades. The distinct merit of this vibration method allows continuous noninvasive on-line monitoring and identification of the transformer problems instantaneously. These advantages attracted many researchers working on this method. García and his group [3] indicated the general relationship of winding vibration with its input voltage and current after a series of vibration tests on a dry power transformer winding without cooling oil. They also provided some convincing evidence showing that the vibration measured from the transformer tank can be used to detect some winding failure modes, such as winding deformation. Similar vibration experimental results and conclusions can be found in other papers [4, 5]. However, considering the practical winding failures, it is reported that about half of failures are caused by the insulation problems [1]. Despite this, it appears that no significant research discussing this winding insulation issue using winding vibration has been conducted. Therefore, this paper focuses on a fundamental research of the effect of winding insulation paper ageing on winding vibration.

Considering the complicated structure of disc-type power transformer winding, this paper aims to understand the effect of insulation paper ageing on the winding's vibration using a relatively simple "winding model" comprising a single layer of concentric circular rings. This is because the disc-type power transformer winding is formed from a series of discs, and each disc can be treated as one layer of concentric circular rings. Because the main exciting electromagnetic force applied on the winding is induced by the current in the winding, most of winding vibration energy is concentrated in the radial direction. Therefore, this paper only discusses the in-plane vibration of the rings.

In the first part of this paper, the mechanical properties of the ageing insulation paper will be mentioned as they are considered to be key influencing parameters in the winding vibration. Then the effect of insulation paper ageing on winding vibration is simulated experimentally by two single layer winding discs with aged paper. Finally, a mechanical model of concentric circular rings is built to explain the experimental phenomena theoretically.

2. AGEING OF WINDING INSULATION PAPER

The power transformer winding comprises of discs formed by several layers of insulation paper wrapped tightly around the winding wire but not solenoid formed. This design is helpful for the winding to undertake large current and provide enough insulation ability. However, winding insulation paper in the serving power transformers is aged over time caused by the internal high electrical and thermal pressures in the transformer tank. The insulation ability of the paper degrades over time, and a winding with "failed" insulation paper could be thoroughly damaged by short circuit accidents. For this reason, the insulation properties of winding insulation paper have been the topic of concern by electrical scholars for a very long time. To define the insulation ability of the paper, the Degree of Polymerisation (DP) is used. It is the average number of glucose units per cellulose molecule. As the paper ages, the polymer chains of the cellulose molecule is cracked so that the DP value decreases. As a result, glucose is degraded to some small molecule products, such as furfuraldehyde or furan. The DP value for new insulation paper is greater than 800. It is believed that when this value is lower than 200, the paper could be defined as "failed" which means its insulation ability is insufficient [6, 7]. Most of the previous research on insulation paper ageing focuses on the electrical properties of the paper with DP changes. This paper, however, is more concerned with the mechanical properties of the ageing paper because it may affect the vibration behavior of the winding.

An accelerating ageing experiment is designed for obtaining the aged paper samples. Several new insulated winding copper wire strips (10cm) are immersed in the transformer's cooling oil in sealed glass bottles. All the bottles are heated to 160℃ in a furnace for between 7 and 34 days. According to Hill's paper [7], the paper at such high temperature should be thoroughly failed (DP<200) in 34 days. After ageing, the strips were taken out of the oil, and dried at 60℃ for 6 hours. Then the paper samples were removed from the wire for the mechanical tests.

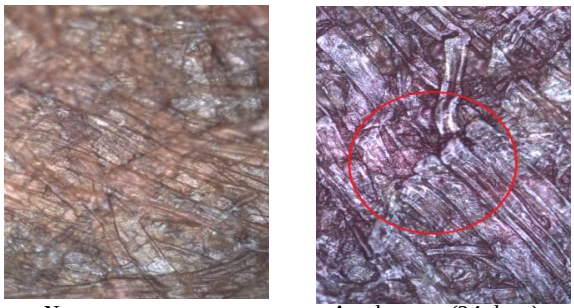

New paper *Aged paper (34 days)*

Figure 1. Cellulose of insulation paper samples before and after the ageing experiment
(sample size approx. 10μm×10 μm)

As mentioned before, when the paper ages, some of the polymer chains of cellulose molecules break. Physically, the breakage can be directly observed by using a microscope. Figure 1 compares the cellulose of the paper before and after the ageing experiment. Although the two pictures come from different paper samples, the phenomena of cellulose are observable almost everywhere in the samples. In the new sample, most of cellulose molecules are unbroken. But some obvious breakages (highlight by the red circle) could be found in the aged paper. As a result, it is logical to infer that the mechanical strength of the paper must change when it ages.

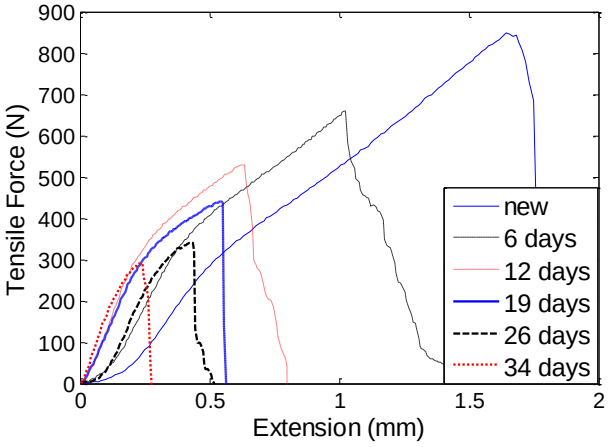

Figure 2: In-plane tensile force of paper

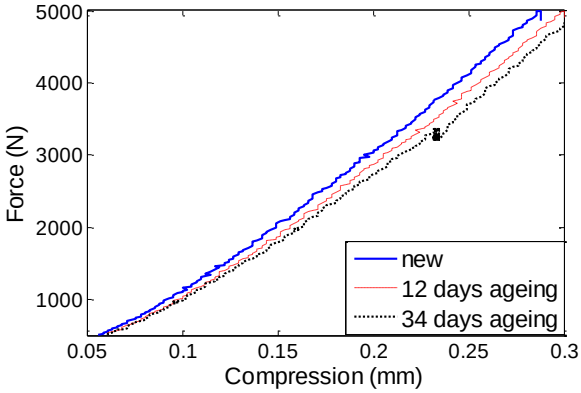

Figure 3: Out-of-plane force/compression curves of paper

Figure 2 shows the in-plane ultimate tensile force of a single layer of paper (area of cross-section approx. 2 mm^2) before it cracks. The paper is clamped at both ends and dragged in opposite directions until it is torn. One clear trend is the ultimate force decreases with the age time. However, another interesting phenomenon is the stiffness of the paper in the in-plane direction does not decreases but increases. A possible explanation for this result is that because the number of polymer chains of cellulose molecule decrease after ageing, the ultimate tensile force the paper can undertake also decrease. However, for each cellulose molecule, it hardens up caused by the high thermal pressure during the ageing test and the cooling processing after the ageing. Similar to cold rolled steel, it becomes stiffer but more brittle. As a result, the in-plane stiffness of the paper increases before the ultimate tensile force point. It also provides another reason why the paper is easy to crack after ageing. On the other hand, Figure 3 gives the force/compression curves for 12 layers of paper (area of cross-section is 340 mm^2) in the out-of-plane direction. For clarity, only the results from the new, 12 days aged and 34 days aged paper are given. From these curves, it is found that the out-of-plane stiffness of the paper (see Table 1) decreases with the ageing time. This phenomenon could be explained by a "Pick Up Sticks" game: A piece of insulation paper consisted of thousands of cellulose molecules can be seen as lots of sticks combined together. For new paper, every stick is relatively long and supported by each other. Therefore the paper is hard to compress and appears stiff. When the paper ages as the cellulose molecules are cracked, each stick breaks into several short sticks, the support effect weakens, and it is easier to compress. When the stiffness change has been explained, a logical supposition is the damping effect of the aged paper may reduce caused by the same ageing phenomenon. The damping of the paper mainly comes from viscous effect between paper cellulose molecules. Because the average contact surface of cracked cellulose molecules is smaller than the perfect cellulose molecules, the viscous effect between them decreases. This means the damping coefficient of the paper should reduce when the paper ages.

3. WINDING DISC WITH AGED INSULATION PAPER

From the results of the previous section, it is clear that the mechanical properties of the insulation paper vary with age. As the paper is one of the main components of the winding, it is supposed that the change in mechanical properties of the insulation paper should affect the winding's mechanical vibration. To investigate this, another accelerating ageing experiment is implemented using winding disc wrapped with insulation paper. As one element of disc-type winding, the results of the winding disc could represent the vibration characteristic of the winding, especially in the radial direction.

Table 1. Ageing properties of the insulation paper

Ageing time	New	6 days	12 days	19 days	26 days	34 days
In-plane ultimate force (N)	862	780	533	447	342	298
In-plane stiffness (10^5N/m)	5.39	7.62	8.46	8.13	7.95	13.2
Out-of-plane average stiffness (10^7N/m)	1.444	1.395	1.359	1.342	1.327	1.325

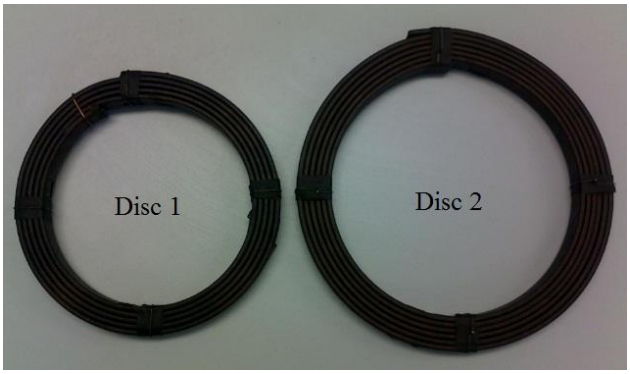

Figure 4. Two winding discs with insulation paper (after the accelerating ageing experiment)

To improve the accuracy of the experiment, two different copper winding discs (Figure 4) are used. The parameters of these discs are listed in Table 2. Similar to the paper ageing experiment, these two discs are immersed in transformer cooling oil in a sealed container. The ageing experiment is performed at 160℃ for a total of 28 days. During the experiment, the vibrations of the discs are measured every 7 days. Before each vibration measurement, the discs are removed from the oil and dried at 60℃ for 6 hours, and then they cool to room temperature.

Table 2. Parameters of tested discs

	Disc 1	Disc 2
Number of turns	5	6
Diameter of outside turn (mm)	161	201
Diameter of inside turn (mm)	133	164
Thickness of tape (mm)	3	3
Width of tape (mm)	15	15
Layers of paper for each turn	4	4

During the vibration experiment, each disc is hung on a metal stand, and excited by a hammer impulse force applied at location θ_0 on the outside turn opposite the hanging point. Then the radial vibration of the disc is collected from several locations θ_1 to θ_N on both the outside and inside turns by accelerometers. It is worthwhile to note that for measuring the vibration of the disc, the accelerometers must be attached on the surface of the copper tape, not on the insulation paper. From experience of former experiment, the disc vibration recorded from the paper is not reliable at all. Therefore, several holes are cut on the insulation paper so that the accelerometers can be fixed on the surface of copper wire directly. Considering that too many holes may affect the mechanical properties of the insulation paper, the disc vibration is only measured at limited locations. Figure 5 represents the vibration measurement setting. The angle between θ_0 and θ_3 is about 5 degrees. For disc 1, the vibration is measurement at locations θ_1 to θ_8. For disc 2, the vibration is only recorded at locations θ_1 to θ_4.

Figure 6 shows the measured radial vibration of each disc at different age times. For clarity, 10dB off-set is applied one by one except the top curve in each diagram. The same experimental features could be observed from different discs or different measurement locations. The main features of the measured vibration are:

1. The natural frequencies of the disc shift to the low frequency end during the ageing process. The details of this shift are given in Table 3 and the top diagram of Figure 7. Besides the same shift trend, the same natural frequency of these two discs shift by a similar extent in percentage, and the movement of the lower order natural frequency is bigger than the higher order one.

2. The frequency band of the disc resonance peaks becomes narrower when the ageing time increases. From Table 3 and the bottom diagram of Figure 7, it is found that the calculated system damping ratios based on *3dB decay method* decrease with the ageing time, especially the first two modes from 7 days to 21days.

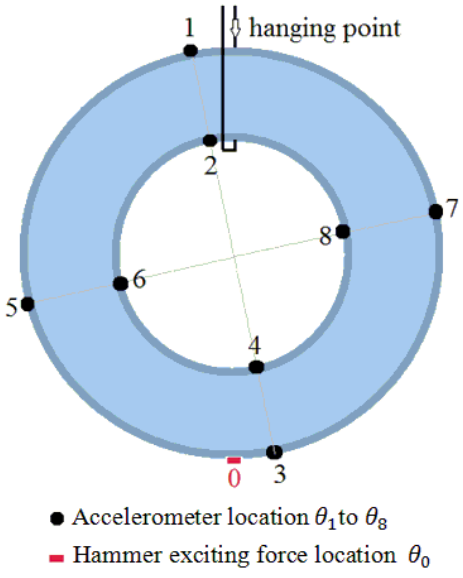

Figure 5. Schematics of vibration measurement setting

At the ageing temperature, 160℃ , the physical properties of copper wire should be stable. All the vibration measurements are implemented at room temperature, so that the geometrical change due to thermal expansion and construction of the copper disc could be negligible. Therefore, it is reasonable to infer that the above experimental phenomena are caused by the ageing of insulation paper. In Section 2, it is known that: the stiffness and the damping coefficient of insulation paper in the out-of-plane direction decreases with the age. Therefore, the system stiffness and damping ratio ξ of the disc with insulation paper also decreases caused by the paper degradation over time. In mechanical sense, we know that the system natural frequencies f should reduce when system stiffness decreases (feature 1). Similarly, when the system damping ratio becomes smaller as the paper ageing, the frequency band of these resonance peaks narrows down (feature 2). However, as these explanations are

based on the general mechanical knowledge, more powerful theoretical evidence should be provided to support the conclusion.

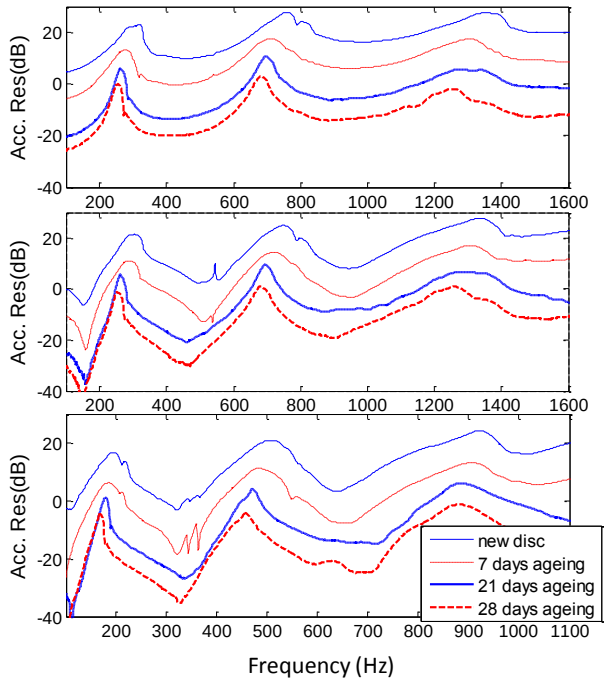

Figure 6. Radial vibrations of winding discs with different aged insulation paper
(top diagram: *disc1, accelerometer location* θ_2; middle diagram: *disc 1, accelerometer location* θ_2;bottom diagram: *disc 2, accelerometer location* θ_3. 10dB off-set is applied to each curve except the top curve for clarity)

Table 3. Natural frequencies and damping ratios of the discs

Ageing time		Natural frequency 1		Natural frequency 2		Natural frequency 3	
		f (Hz)	ξ*	*f* (Hz)	ξ*	*f* (Hz)	ξ*
New	Disc1	301	0.097	750	0.052	1337	0.048
	Disc2	194	0.085	510	0.075	925	0.046
7 days	Disc1	292	0.094	723	0.059	1306	0.052
	Disc2	188	0.105	492	0.068	905	0.053
21 days	Disc1	263	0.044	697	0.027	1292	0.073
	Disc2	179	0.042	474	0.028	883	0.050
28 days	Disc1	258	0.045	684	0.032	1263	0.045
	Disc2	169	0.036	455	0.029	877	0.047

*Based on *3dB decay method*, the damping ratio can be calculated by $\xi = \frac{\triangle f}{2f_r}$, where Δf is the bandwidth of 3dB decay, f_r is the resonance frequency.

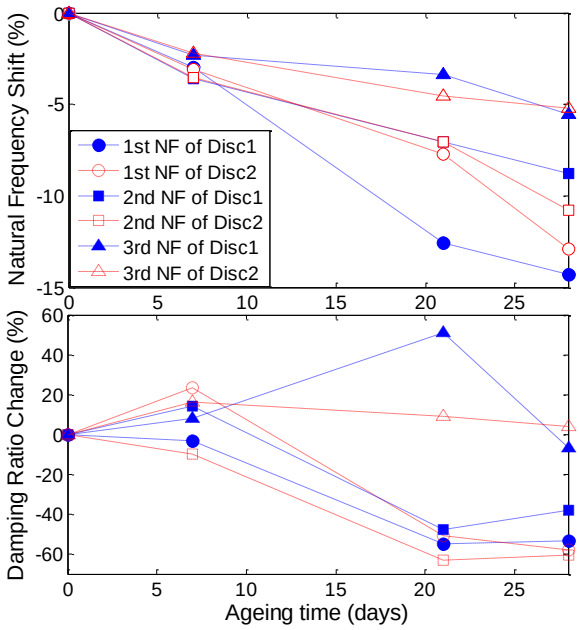

Figure 7. Natural frequency shift (top) and damping ratio change (bottom) of the discs with different ageing times

4. MODELLING OF RINGS

In order to give some theoretical explanations for the disc experiment, a preliminarily winding disc model is built and discussed in this section. As mention before, a single layer winding disc could be approximately modelled as a series of concentric circular rings. For clarity, the model of a single ring is given first in this section. Then this single ring model can be extended to concentric circular rings.

4.1 SINGLE RING MODEL

The vibration of a ring has been researched since the 1920s. Love gave the first single ring model in his book "*A Treatise on the Mathematical Theory of Elasticity*" [8]. But his model is limited to circular cross-section and neglects shear deflections. Since then lots of researchers have strived to improve this model. Regarding to the practical disc used in the experiment, focus is directed to the in-plane vibration of a thin ring with rectangle cross-section in this paper.

Based on the *elastic theory*, the in-plane vibration of a single ring could be described by following five equations [9]:

$$\rho Aa\frac{\partial^2 U}{\partial t^2} = \frac{\partial P}{\partial \theta} - Q\,, \tag{1}$$

$$\rho Aa\frac{\partial^2 V}{\partial t^2} = \frac{\partial Q}{\partial \theta} + P, \tag{2}$$

$$\frac{\partial M}{\partial \theta} - Pa = \rho Ak_z^2\frac{\partial^2}{\partial t^2}\left(V - \frac{\partial U}{\partial \theta}\right), \tag{3}$$

$$Q = \frac{EA}{a}\left(U + \frac{\partial V}{\partial \theta}\right), \tag{4}$$

$$M = \frac{EAk_z^2}{a^2}\left(\frac{\partial V}{\partial \theta} - \frac{\partial^2 U}{\partial \theta^2}\right), \tag{5}$$

where (*U, V) and* (*P, Q*) are the displacements and resultant forces in the radial and tangent direction respectively; *M* and k_z are torque and area radii of gyration of the cross-section in the axial direction; *a, E,* ρ , and *A* are the radius, Young's modulus, density and area of cross-section of the ring, respectively.

Based on the *Modal Expansion Method*, the vibration of a structure could be treated as the superposition of its infinite modes. For the uniform ring, its in-plane mode shape functions can be written as [10]:

$$U = \sum_{m=1}^{\infty} C_{1m} \sin(m\theta) e^{j\omega t}, \tag{6}$$

$$V = \sum_{m=1}^{\infty} C_{2m} \cos(m\theta) e^{j\omega t}. \tag{7}$$

Substituting Equation (4) into Equation (2) and using the mode shape functions (6) and (7), yields

$$P = -\omega^2 \rho A a V - \frac{EA}{a}\frac{\partial U}{\partial x} + \frac{EAm^2}{a} V. \tag{8}$$

Similarly, extracting *P* again by substituting Equations (5), (6) and (7) into Equation (3) gives

$$P = \left(\frac{EAm^2 k_z^2}{a^3} - \frac{\omega^2 \rho A k_z^2}{a} \right) \left(\frac{\partial U}{\partial \theta} - V \right). \tag{9}$$

When the external force $F = F_0 \delta(\theta - \theta_0) e^{j\omega t}$ at loctation θ_0 is not zero, by combining Equations (8) and (9), we obtain the in-plane vibration equation of the ring as

$$W_1 V - W_2 \frac{\partial U}{\partial \theta} = \frac{a^3}{A} F, \tag{10}$$

where

$$W_1 = -\omega^2 \rho a^4 + E a^2 m^2 + E m^2 k_z^2 - \omega^2 \rho a^2 k_z^2,$$

$$W_2 = E a^2 + E m^2 k_z^2 - \omega^2 \rho a^2 k_z^2.$$

However, there are two unknown variables C_{1m} and C_{2m} in Equation (10). To solve the Equation (10), differentiating Equation (2) with respect to θ, eliminating *P* between the resulting equation and Equation (1), and using Equation (4) to eliminate *Q* gives:

$$\rho a^2 \frac{\partial^2}{\partial t^2} \left(\frac{\partial V}{\partial \theta} - U \right) = E \left(\frac{\partial^2}{\partial \theta^2} + 1 \right) \left(U + \frac{\partial V}{\partial \theta} \right). \tag{11}$$

Expanding Equation (11) by using the mode shape functions (6) and (7), gives

$$C_{2m} = -\frac{W_3}{m} C_{1m}, \tag{12}$$

where $W_3 = \dfrac{\omega^2 \rho a^2 + E\left(m^2 - 1\right)}{\omega^2 \rho a^2 - E\left(m^2 - 1\right)}$.

Substituting Equations (6) and (7) into Equation (10), and using Equation (12) and orthogonal relationships between the mode shapes, we obtain the model coefficient

$$C_{1m'} = -\frac{F_0 m a^3 \cos(m'\theta_0)}{A\pi (W_1 W_3 + m^2 W_2)}, \tag{13}$$

which together with Equation (12) yields the system response.

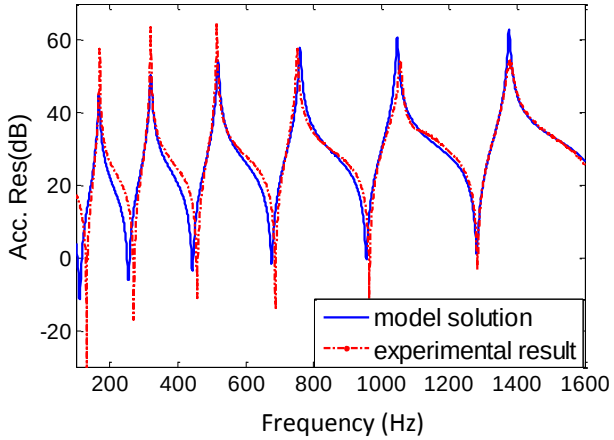

Figure 8. Radial vibration of a single ring at location θ_3

To confirm the reliability of the model, a comparison experiment of a copper ring is implemented. The diameter of the ring is 300 mm, and the remaining parameters of the ring can be found in Table 2. The experiment setting is the same with the disc experiment. From Figure 8, it is obvious that the model solution (in-plane vibration response of the ring) agrees highly with the experimental result. The small difference may be caused by the error in the value for the copper Young's modulus and the geometric structure of the ring being imperfect.

4.2 CONCENTRIC RINGS MODEL WITH INSULATION PAPER

The next step is to extend the single ring model to build a preliminary model of concentric circular rings with insulation paper to reconstruct to the phenomena in the disc experiment and explain them. To describe the role of insulation paper in the model, it is assumed that every two adjacent rings are coupled by the insulation paper between them. Because the paper distribution is uniform between rings, it can be divided into *N* finite elements at corresponding locations θ_1 to θ_N, and each element could be modelled as a spring-damper system (see Figure 9). For clarity, only the simplest model, three rings with one element, is demonstrated here. The result can be easily extended to *Z* rings with *N* paper elements, where *Z* and *N* are arbitrary integers.

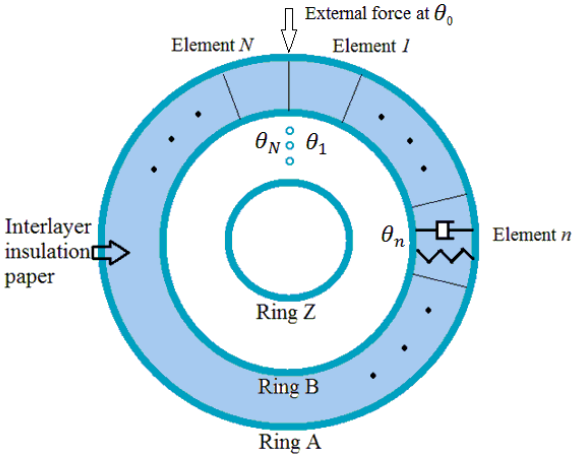

Figure 9. Theoretical model of concentric circular rings with insulation paper

Still assuming the external force is applied on the outside ring (Ring A) at location θ_0, and the element is at location θ_1, the vibration equations of these three rings are:

$$W_{A1}V_A - W_{A2}\frac{\partial U_A}{\partial \theta} = \frac{a_A^3}{A}F_A, \tag{14}$$

$$W_{B1}V_B - W_{B2}\frac{\partial U_B}{\partial \theta} = \frac{a_B^3}{A}F_B, \tag{15}$$

$$W_{C1}V_C - W_{C2}\frac{\partial U_C}{\partial \theta} = \frac{a_C^3}{A}F_C, \tag{16}$$

where

$$F_A = F_0\delta(\theta-\theta_0) - (k_p + j\omega C_p)[U_A(\theta_1) - U_B(\theta_1)]\delta(\theta-\theta_1),$$

$$F_B = (k_p + j\omega C_p)[U_A(\theta_1) - U_B(\theta_1)]\delta(\theta-\theta_1) - (k_p + j\omega C_p)[U_B(\theta_1) - U_C(\theta_1)]\delta(\theta-\theta_1),$$

$$F_C = (k_p + j\omega C_p)[U_B(\theta_1) - U_C(\theta_1)]\delta(\theta-\theta_1).$$

All the symbols represent the same parameters of the single ring model with a subscript that indicates the different rings. k_p and C_p represent the unit out-of-plane stiffness and damping coefficient of each paper element. After a similar process to the single ring model, Equations (14) to (16) can be rewritten as

$$-\pi\left(\frac{W_{A1}W_{A3}}{m'} + m'W_{A2}\right)C_{A1m'} + \frac{a_A^3(k_p + j\omega C_p)}{A} \cos(m'\theta_1)[\sum_{m=1}^{\infty}\sin(m\theta_1)(C_{A1m} - C_{B1m})] = \frac{a_A^3}{A}F_0\cos(m'\theta_0), \tag{17}$$

$$-\pi\left(\frac{W_{B1}W_{B3}}{m'} + m'W_{B2}\right)C_{B1m'} - \frac{a_B^3(k_p + j\omega C_p)}{A} \cos(m'\theta_1)[\sum_{m=1}^{\infty}\sin(m\theta_1)(C_{A1m} - 2C_{B1m} + C_{C1m})] = 0, \tag{18}$$

$$-\pi\left(\frac{W_{C1}W_{C3}}{m'} + m'W_{C2}\right)C_{C1m'} - \frac{a_C^3(k_p + j\omega C_p)}{A} \cos(m'\theta_1)[\sum_{m=1}^{\infty}\sin(m\theta_1)(C_{B1m} - C_{C1m})] = 0. \tag{19}$$

In the practical model calibration, only finite number of M modes are used. Therefore, Equations (17) to (19) could be expanded to $3\times M$ independent equations with $3\times M$ variables C_{A11} to C_{C1M}, which are solvable.

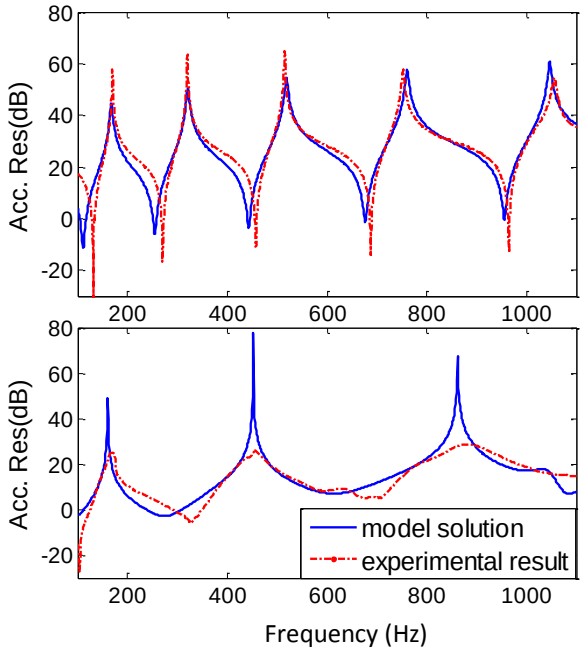

Figure 10. The comparison of the concentric rings model solutions with experimental results

Figure 10 compares the solutions of this concentric rings model with the experimental results. The model solutions, which are obtained from 6 rings and 100 paper elements model, simulate the disc vibration at the outside location θ_3 in the experiment (see Figure 5). The top diagram indicates this model is able to describe the vibration of the single ring accurately when assuming the k_p and C_p equal to zero which means the outside ring loses all its coupling effect and vibrates as a single ring. The bottom diagram tries to reconstruct the vibrations of disc 2 with aged paper. Although there are some obvious amplitude differences, the model solution provides close values of these natural frequencies with the experimental result. To further check the correctness of this concentric rings model, Figure 11 compares the first two mode shapes of the disc. The blue circle is the calculated shape from the model, and the red points are the measured result of the experiment. The coordinate points 0º, 90º, 180º and 270º are corresponding to the measurement points θ_3, θ_7, θ_1 and θ_5 respectively in the experiment (see Figure 5). The first mode shape is in great agreement. For the second mode, although some differences exist between the model and experiment, the overall mode shape is also quite similar.

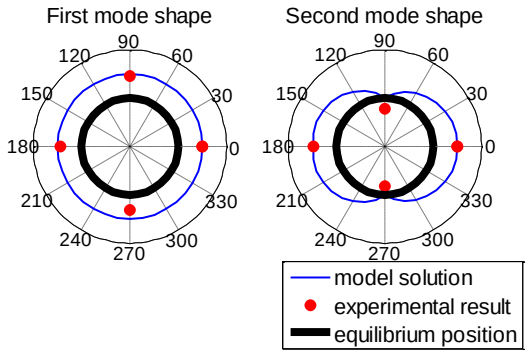

Figure 11. The normalised mode shapes of the first two modes of the disc 1

According to above comparison, it is reasonable to say that this preliminary concentric circular rings model is able to describe some mechanical characteristics of the winding disc. Figure 12 plots the model solutions using different paper parameters k_p and C_p to simulate the disc 2 with new and ageing paper. For clarity, the figure focuses on the third natural frequency. The blue curve represents the new disc with paper parameters $k_p=1.44\times10^7$ N/m and $C_p=10$ Ns/m. The red curve represents the aged disc whose paper parameters are ten times smaller than the blue curve. The natural frequency of the disc shifts to the low frequency end when the mechanical properties of the insulation paper decrease representing the ageing of the winding insulation paper. This trend was also observed experimentally.

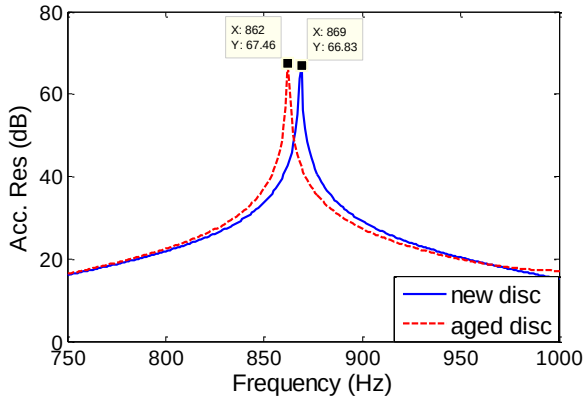

Figure 12. Theoretical simulation of winding disc 2 with new and aged insulation paper

Two problems of this concentric rings model are worth discussing here. On one hand, the model cannot explain the damping effect in the experiment. Based on the model, it seems that the damping change of the paper hardly affects the disc vibration. As a result, the model solution has much narrower resonance peaks than the experimental result, and the frequency band of these peaks does not change with different paper damping values. On the other hand, although the model and experiment show the same shift direction of the natural frequencies while the paper is ageing, the sensitivity of the model is much less. The most likely reason for these differences is the limitations of model itself. The winding discs are made as spiral type, but this preliminary model uses concentric circular rings. Whether this method can fully describe the mechanical characteristics of the winding disc or not needs more research. Another limitation is the paper is only modelled in its out-of-plane direction (the radial direction of the disc). However, the in-plane vibration of the disc is determined by both radial force and tangent force which means the paper should be modelled in its in-plane direction as well to describe its effect in the tangent direction of the disc vibration. The in-plane mechanical properties of the paper may include the in-plane stiffness of the paper and the friction between paper layers. The friction introduced by the paper can be a part of, or even the main part of system damping in the disc. Therefore, when the paper effect in tangential direction of the disc is included, the accuracy of the model may be highly improved.

5. CONCLUSIONS AND FURTHER WORK

Ageing of winding insulation paper is one of the most serious power transformer failures. This paper provides some experimental and theoretical evidence supporting that the vibration characteristics of the winding disc is affected by the mechanical properties of the insulation paper that vary with ageing extent. Specifically, when the paper ages, the mechanical properties of the paper in its out-of-plane direction decrease. As a result, the natural frequencies of winding disc shift to low frequency end. This research reveals a potential possibility that the ageing extent of winging insulation paper can be detected by monitoring the winding's mechanical vibration.

The further work of this research will focus on two aspects. One is improving the accuracy of the existing concentric circular rings model. The difference between the spiral disc and concentric rings will be simulated by FEM as it is difficult to achieve this experimentally because of the inevitable errors, such as the geometrical error of the tested items due to the manufacture procedure. Meanwhile, a more accurate rings model will be developed by introducing the paper effect in the tangential direction of the disc. The other aspect of the further research is building a multilayer disc model that is closer to actual disc-type winding. Experiments to analyse some other winding failure modes, such as loss of winding clamping pressure and winding partial deformation will also be performed.

ACKNOWLEDGEMENTS

We thank Dr. Andrew Guzzomi for proof reading the manuscript and useful suggestions. Financial support to this project by CRC for Infrastructure Engineering Asset Management (CIEAM) is gratefully acknowledged.

REFERENCE

[1] M. Wang, et al., "*Review of condition assessment of power transformers in service*", IEEE Electrical Insulation Magazine, 2002, Vol 18, No. 6, pp. 12-25.

[2] CIGRE Working Group 05, "*An international survey on failures in large power transformers in service*", Electra, 1983, No. 88.

[3] B. García, et al., "*Winding deformations detection in power transformers by tank vibration monitoring*", Electric Power System Research 74, 2005, pp. 129-138.

[4] S. C. Ji, "*Failure Monitoring Investigation of Transformer Wingding and Core Characteristic*", Xi An Jiao Tong University, 2003.

[5] Z. Berler, et al., "*Vibro-Acoustic Method of Transformer Clamping Pressure Monitoring*", Conference Record of the 2000 IEEE International Symposium, pp. 263 – 266.

[6] T. K. Saha and P. Purkait, "*Understanding the impacts of moisture and thermal ageing on transformer's insulation*

dielectric response and molecular weight measurements", IEEE Transactions on Dielectrics and Electrical Insulation, 2008, Vol. 15, N0. 2, pp. 568-582.

[7] D. J. T. Hill, "*A study of degradation of cellulosic insulation materials in a power transformer, part 1. Molecular weight study of cellulose insulation paper*", Polymer Degradation and Stability 48, 1995, pp. 79-87.

[8] A. E. H. Love, "*A Treatise on the Mathematical Theory of Elasticity*", New York Dover Publications, 1927.

[9] T. Charnley, et al., "*Vibrations of thin rings of rectangular cross-section*", Journal of Sound and Vibration, 1989, Vol. 134, Issue 3, pp. 455-488.

[10] V. I. Lazarev and V. E. Rushchak, "*Equations of circular-ring oscillations*", Plenum Publishing Corporation, 1983, pp. 1683-1687.